IJREAT International Journal of Research in Engineering & Advanced Technology, Volume 3, Issue 4, Aug-Sept, 2015
ISSN: 2320 – 8791 (Impact Factor: 2.317)
www.ijreat.org

A Parametric Study Of Solidification Of PCM In An Annulus With Alternating Fins

Kamal A. R. Ismail[1], Monica M. Gonçalves[2], Fatima A. M. Lino[3]

[1,2,3]Department of Energy, Faculty of Mechanical Engineering, State University of Campinas,
UNICAMP, Mendeleiev street, 200, Cidade Universitária "Zeferino Vaz", Postal Code 13083-860, Campinas (SP), Brazil.

Abstract

This paper presents the results of a numerical study on internally and externally finned annulus in which the internal tube has external fins while the external tube has internal fins. This arrangement is investigated with the objective of increasing the heat transfer rate, reducing the time for complete phase change and allowing for simultaneous charging and discharging processes. The proposed model is based upon pure conduction in the PCM and is solved by the control volume method and the finite difference scheme. To establish the validity of the model, the results were compared with available data. Additional results were presented to show the influence of the size of the PCM annular gap, the number of fins and the fin length.

Keywords: *Solidification, PCM, Axially Finned Tube, Energy Storage.*

1. Introduction

Commercial acceptance and the economics of solar thermal technologies are tied to the design and development of efficient, cost-effective thermal storage systems. Thermal storage units that utilize latent heat storage materials have received greater attention in the recent years because of their large heat storage capacity and their isothermal behavior during the charging and discharging processes.

Thermal energy storage such as latent heat thermal energy storage can reduce the energy supply–demand mismatch and improve the efficiency of thermal energy systems because of its high thermal energy density per unit mass and per unit volume. It is generally preferred to sensible heat storage because of the high storage capacity and the nearly constant temperature during the charging and discharging processes. It is important to remember that most phase-change materials (PCM) with high energy storage density have a low thermal conductivity and hence heat transfer enhancement techniques are required for any latent heat thermal storage. Irrespective of these thermal merits latent heat storage is hindered by its low thermal conductivity which impairs heat transfer from the PCM or to it. Many studies were devoted to improve the effective

thermal conductivity of the PCM by submersing metallic screens in the PCM, metallic powders, fins and many other techniques. A great deal of finned geometries was investigated both numerically and experimentally for a variety of applications and at different temperature levels. The presence of fins increases the heat transfer area, permits extending the heat transfer surface within the PCM mass besides reducing the undesirable convection effects during melting the PCM.

Finned geometries were investigated with the objective of reducing the undesired effects of natural convection and increase the heat transfer rate by Kalhori and Ramadhyani [1] and Sasaguchi et al. [2]. A numerical study on an axially finned tube spanning the cylindrical annulus was realized by Padmanabhan and Murthy [3]. Their model assumes pure conduction and the equations were solved by finite difference approach. Ismail and Alves [4] and Ismail and Gonçalves [5] studied the phase change around axially finned tubes submersed in the PCM. Some studies were realized on finned tube both numerically and experimentally as in Choi and Kim [6], Lacroix [7], Choi and Kim [8], Choi et al. [9], Zhang and Faghri [10], Velraj et al. [11] and Ismail et al. [12].

The recent and urgent needs of ambient protection and preservation of natural resources to avoid further degradation of the environment by both emissions and wastes and depletion of natural resources, intensified research efforts dedicated to sustainable solutions for the diverse aspects of energy production and utilization. These efforts resulted in cost reduction of energy based on renewable resources allied with sustainability and liability. In such applications energy storage is a vital piece linking

the energy source to the energy demand. Among the different options of thermal energy storage latent heat storage is top ranked due to its numerous merits. In recent years many studies were devoted to aspects of modeling and numerical treatment of phase change problems. Full scale projects, pilot studies and experimental investigations to support the numerical studies were also reported. Techniques like enthalpy methods, finite difference approach, finite element, NTU-e based methods and CFD were used to treat heat transfer elements in the form of bare tubes, internally finned tubes, externally finned tubes and coiled tube systems. Among these studies one can cite [13-18].

Most of the latent heat storage materials have low thermal conductivity, a fact which negatively reflects on the charging and discharging heat flow rates impairing the thermal performance of the latent heat storage unit. Many methods were tried to enhance the thermal conductivity of the PCM, among the effective and cheap methods one can include micro metallic powders dispersed in the PCM, and finned tubes of different geometrical arrangements [19-22].

Shokouhmand and Kamkari [23] presented a numerical investigation on the melting of phase change material using paraffin wax inside a double pipe heat exchanger. Numerical simulations were performed for melting of PCM in annulus where the inner pipe has two or four longitudinal fins. The results compared with those of a bare tube showed that melting performance of PCM significantly improved by using longitudinal fins on the inner tube.

Anisur et al. [24] emphasized the opportunities for energy savings and green house gas emissions reduction with the implementation of PCM in thermal energy storage systems. About 3.43% of CO2 emission by 2020 could be reduced through the application of PCM in building and solar thermal power systems. Similarly, energy conservation and green house gas emissions reduction by other PCM applications are also presented. Thermal energy storage system with phase change material is a potential candidate for mitigating the problem of green house gas emissions and energy conservation.

Chiu and Martin [25] carried a performance analysis of two latent heat thermal storage systems configurations. Charging and discharging rates of a single PCM is compared with multistage system using a cascade of multiple PCM at various phase change temperatures in a submerged finned pipe heat exchanger. The work was conducted with a finite element based numerical simulation.

Basal and Unal [26] presented an investigation on thermal energy storage system of a triple concentric-tube arrangement to achieve performance enhancement. A numerical study was conducted by using enthalpy method to investigate the effects of mass flow rate, the inlet temperature of the heat transfer fluid and the variation of the tubes radii on the system performance. The results indicate a significant enhancement in the system performance.

Al-abidi et al. [27] investigated numerically heat transfer enhancement by using internal and external fins for PCM melting in a triplex tube heat exchanger. A two-dimensional numerical model was developed using the Fluent 6.3.26 software program. The number of fins, fin length, fin thickness, Stefan number, triplex tube heat exchanger material, and the latent heat storage unit geometry were found to influence the time for complete melting of the PCM.

The present paper reports the results of a numerical study on internally and externally finned annulus in which the internal tube has external fins while the external tube has internal fins. This arrangement is investigated with the objective of increasing the heat transfer rate, reducing the time for complete phase change and allowing for simultaneous charging and discharging processes. The proposed model based on pure conduction in the PCM is discretized by the control volume method and the finite difference approximation. The numerical predictions are compared with available results to establish the validity of the model. Additional results are obtained to show the influence of the size of the PCM annular gap, the number of fins and the fin length.

2. Formulation of the Problem

Fig. 1 shows a section of the finned tubes system, the flow passage of the heat transfer fluids and the external insulation layer. As can be seen the internal tube has external fins while the external tube is fitted with internal fins. The space between the two tubes is occupied by the PCM. By this arrangement it is possible to enhance the heat transfer charging and discharging processes. If it is required to charge and discharge the unit this will be possible by arrangement of a system of valves to allow one

fluid passing in the internal tube and another fluid retrieving the stored energy by flowing in the external tube. It is also possible to have few units of this type forming a multi tube bigger storage unit. In this case the insulation layer will be represented in the model by the symmetry circle or adiabatic section after which there is no heat transfer as can be seen in Fig. 2.

The energy equation for the multidimensional phase change problem, under the assumptions of no compressibility, no viscous effects, negligibly small velocity components, no internal heat generation and constant density, can be written in the form

$$\frac{\partial \overline{H}(T)}{\partial t} = \nabla \cdot (k(T).\nabla T) \tag{1}$$

where T is the temperature, k is the thermal conductivity and ρ is the specific mass.

The enthalpy $\overline{H}(T)$ per unit volume can be written in terms of temperature as suggested by Bonacina et al. [28]

$$\overline{H}(T) = C(T)dT + \lambda\delta(T - T_m) \tag{2}$$

where C(T) and λ are the thermal capacity and the latent heat per unit volume respectively and δ(T-T_m) is the Dirac function. As the enthalpy is function of the thermal capacity, one can write

$$\overline{C}(T) = \frac{d\overline{H}(T)}{dt} \tag{3}$$

where $\overline{C}(T)$ is the equivalent thermal capacity per unit volume. Hence the energy equation can be written in the form

$$\overline{C}(T)\frac{\partial T}{\partial t} = \nabla \cdot (k(T).\nabla T) \tag{4}$$

$$\int_{T_m^-}^{T_m^+} \overline{C}(T)dT = \lambda + \int_{T_m^-}^{T_m} C_s(T)dT + \int_{T_m}^{T_m^+} C_l(T)dT \tag{5}$$

resulting in

$$\overline{C}(T)\left(T_m^+ - T_m^-\right) = \lambda + C_s(T)\left(T_m - T_m^-\right) + C_l(T)\left(T_m^+ - T_m\right) \tag{6}$$

where $\left(T_m^+ - T_m^-\right) = 2\left(T_m - T_m^-\right) = 2\left(T_m^+ - T_m\right)$ (7)

Rearranging the above equation one can write

$$\overline{C}(T) = \frac{\lambda}{\left(T_m^+ - T_m^-\right)} + \frac{C_s(T) + C_l(T)}{2} \tag{8}$$

and the equivalent thermal capacity can be finally written in the form

$$\overline{C}(T) = \begin{cases} C_s(T) & T < T_m^- \\ C_l(T) & T > T_m^+ \\ \dfrac{\lambda}{2\Delta T} + \dfrac{C_s(T) + C_l(T)}{2} & T_m^- \le T \le T_m^+ \end{cases} \tag{9}$$

In a similar manner the thermal conductivity can be written in the form:

$$\overline{k}(T) = \begin{cases} k_s(T) & T < T_m^- \\ k_l(T) & T > T_m^+ \\ k_s(T) + \dfrac{k_l(T) - k_s(T)}{2\Delta T}\left(T - T_m^-\right) & T_m^- \le T \le T_m^+ \end{cases} \tag{10}$$

Considering the present problem and the geometrical parameters defined in Figs. 1 and 2, the energy equation can be written in the form:

$$\overline{C}(T)\frac{\partial T}{\partial t} = \frac{1}{r}\frac{\partial}{\partial r}\left(r\overline{k}(T)\frac{\partial T}{\partial r}\right) + \frac{1}{r}\frac{\partial}{\partial \phi}\left(\frac{\overline{k}(T)}{r}\frac{\partial T}{\partial \phi}\right) \tag{11}$$

(3)

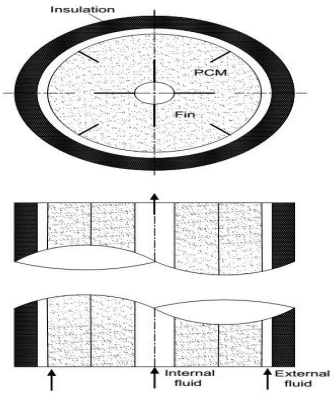

Fig. 1 Geometry of the storage unit with alternating fins.

In the fin region one must use the fin thermal properties as

$$\overline{C}(T) = \rho_a c_a$$
$$\overline{k}(T) = k_a \tag{12}$$

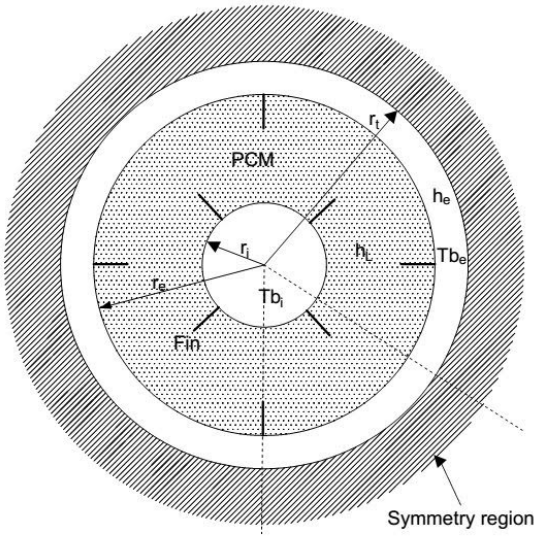

Fig. 2 Details of the geometry of the tube and fins.

The boundary and initial conditions of the problem are specified as

For r = r_i

$$\left.\frac{\partial T}{\partial r}\right|_{r=r_i} = -\frac{h_i}{k(T)}\left[T_{bi} - T(r_i,t)\right] \tag{13}$$

For r = r_e

$$\left.\frac{\partial T}{\partial r}\right|_{r=r_e} = -\frac{h_e}{k(T)}\left[T(r_e,t) - T_{be}\right] \tag{14}$$

For $\phi = 0$

$$\left.\frac{\partial T}{\partial \phi}\right|_{\phi=0} = 0 \tag{15}$$

For $\phi = \phi_e$

$$\left.\frac{\partial T}{\partial \phi}\right|_{\phi=\phi_e} = 0 \tag{16}$$

The initial conditions are specified for different possible situations as below

- The PCM is initially in the liquid state

$$T(r,\phi,t) \geq T_m^+ = T_{m+\Delta T} \tag{17}$$

- The PCM is initially in the solid state

$$T(r,\phi,t) \leq T_m^- = T_{m-\Delta T} \tag{18}$$

In order to generalize the problem and be able to investigate a wide range of parameters the dimensionless variables listed below are used

$$\theta = \frac{T - T_m}{T_m}, \quad R = \frac{r}{\left(r_e^2 - r_i^2\right)^{1/2}}, \quad Fo = \frac{k_s t}{C_s\left(r_e^2 - r_i^2\right)}$$

$$\tilde{C} = \frac{\overline{C}}{C_s}, \qquad \tilde{k} = \frac{\overline{k}}{k_s}, \qquad C_{as} = \frac{\rho_a c_a}{C_s}$$

$$k_{as} = \frac{k_a}{k_s}, \qquad Ste = \frac{C_s\left(T_m^+ - T_{bi}(0)\right)}{\lambda} \tag{19}$$

The dimensionless equivalent thermal capacity per unit volume is

$$\tilde{C}(\theta) = \begin{cases} 1 & \theta < \theta_m^- \\ C_l(\theta)/C_s(\theta) & \theta > \theta_m^+ \\ \dfrac{1}{Ste}\left(\dfrac{\theta_m^+ - \theta_{io}}{\theta_m^+ - \theta_m^-}\right) + \dfrac{C_s(\theta) + C_l(\theta)}{2C_s} & \theta_m^- \leq \theta \leq \theta_m^+ \end{cases}$$

and the dimensionless thermal conductivity is

$$\tilde{k}(\theta) = \begin{cases} 1 & \theta < \theta_m^- \\ k_l(\theta)/k_s(\theta) & \theta > \theta_m^+ \\ 1 + \dfrac{k_l(\theta) - k_s(\theta)}{2k_s}\left(\dfrac{\theta - \theta_m^-}{\theta_m - \theta_m^-}\right) & \theta_m^- \leq \theta \leq \theta_m^+ \end{cases}$$

The energy equation in terms of the new variables can be written in the form

$$\tilde{C}(\theta)\frac{\partial\theta}{\partial Fo}=\frac{1}{R}\frac{\partial}{\partial R}\left(R\tilde{k}(\theta)\frac{\partial\theta}{\partial R}\right)+\frac{1}{R}\frac{\partial}{\partial\phi}\left(\frac{\tilde{k}(\theta)}{R}\frac{\partial\theta}{\partial\phi}\right) \quad (20)$$

The boundary conditions in their dimensionless form are presented as below

$$\left.\frac{\partial\theta}{\partial R}\right|_{R=R_1}=\frac{Bi_i}{R_1}\left[\theta-\theta_{i0}\right] \quad (21a)$$

$$\left.\frac{\partial\theta}{\partial R}\right|_{R=R_2}=-\frac{Bi_e}{R_2}\left[\theta-\theta_{e0}\right] \quad (21b)$$

$$\left.\frac{\partial\theta}{\partial\phi}\right|_{\phi=0}=0 \quad (21c)$$

$$\left.\frac{\partial\theta}{\partial\phi}\right|_{\phi=\phi_e}=0 \quad (21d)$$

where $Bi_i=\frac{h_i r_i}{k}$, $Bi_e=\frac{h_e r_e}{k}$, $R_1=\frac{r_i}{\left(r_e^2-r_i^2\right)^{1/2}}$,

$R_2=\frac{r_{ei}}{\left(r_e^2-r_i^2\right)^{1/2}}$

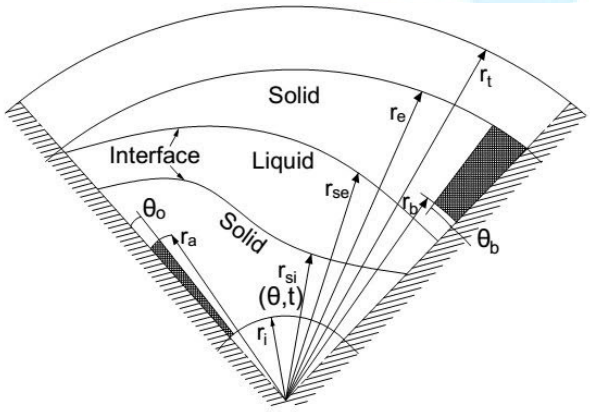

Fig. 3 Variables and details of the symmetry region of the phase change problem.

The initial conditions are specified for different possible situations as below

- The PCM is initially in the liquid phase

$$\theta(R,\phi,0)\geq\theta_m^+ \quad (22)$$

- The PCM is initially in the solid phase

$$\theta(R,\phi,0)\leq\theta_m^- \quad (23)$$

The above system of equations and the associated boundary and initial conditions describes only the phase change problem. This phase change problem is provoked by the flowing fluid (or fluids) in the internal and external tubes as can be seen in Fig.4.

To complete the formulation of the problem it is necessary to couple the phase change problem with the flow problem in the internal and external tube. The coupling of the phase change problem with the fluid flow problem in the internal and external tubes is realized by an energy balance on a control volume of axial length elementary along the flow direction. As was mentioned before it is possible to have the same fluid flowing in the external and internal tubes during the charging and discharging processes.

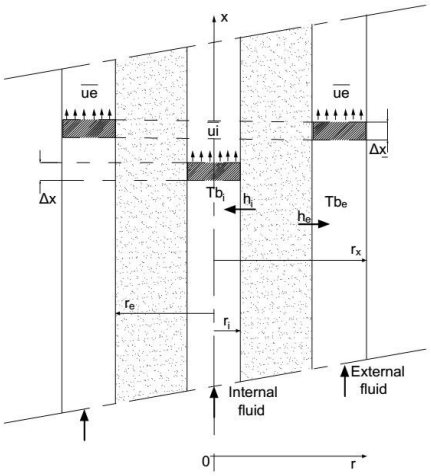

Fig. 4 Details of the flow and phase change problem.

Alternatively it is possible to have a charging fluid flowing into the internal tube and another discharging fluid flowing into the external tube. In this last case the storage system is being charged and discharged simultaneously.

Figure 5 shows the elementary volume including the inner tube and the PCM over which an energy balance is realized

omitting the term $\frac{\partial T_b}{\partial t}$ in relation to the other terms for being small in comparison with the phase change time, one can write

$$\dot{m}_{bi} c_{bi} \frac{dT_{bi}}{dx} = -\dot{q}_i \tag{24}$$

where $\dot{m}_{bi} = A\rho v = \rho_i \pi r_i^2 \bar{u}_i$ and $\dot{q}_i = 2\pi r_i k_s \left.\frac{\partial T}{\partial r}\right|_{r_i}$

The maximum possible energy transfer rate per unit length is

$$\dot{q}_{\max} = 2\pi r_i h_i \left(T_{bi}(t,0) - T_{be}(t,0)\right) \tag{25}$$

while the dimensionless energy transfer to the internal fluid is

$$\bar{q}_i = \frac{\dot{q}_i}{\dot{q}_{\max}} = \frac{\dot{q}_i}{2\pi r_i h_i \left(T_{bi} - T_{be}\right)} \tag{26}$$

By simple mathematical manipulation one can write

$$\frac{dT_{bi}}{dx} = -\frac{\dot{q}_i}{\dot{m}_{bi} c_{bi}} = -\frac{1}{\rho \pi r_i^2 \bar{u}_i} \frac{1}{c_{bi}} \dot{q}_i \tag{27}$$

and $\dot{q}_i = 2\pi r_i h_i \left(T_{bi} - T_{be}\right) \bar{q}_i$ where $T_{bio} = T_{bi}(0)$, $T_{beo} = T_{be}(0)$.

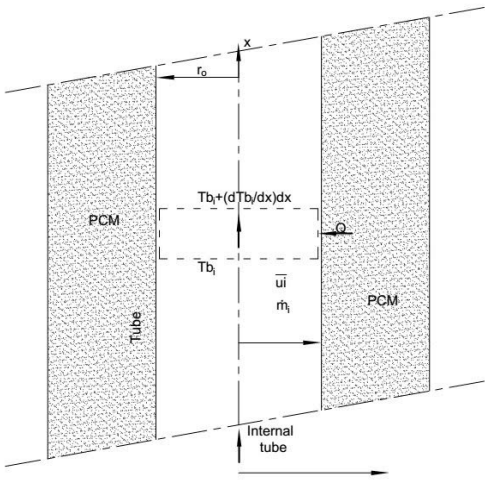

Fig. 5 Details of the flow and phase change problem for the internal fluid.

Eq. (27) can be alternatively written in the form

$$\frac{dT_{bi}}{dx} = -\frac{2h_i \left(T_{bi} - T_{be}\right)}{\rho r_i \bar{u}_i c_{bi}} \bar{q}_i \tag{28}$$

where $\bar{u}_i = \frac{dx}{dt}$ and consequently Eq. (28) can be written in the form

$$\frac{dT_{bi}}{dx} = -\frac{2h_i \left(T_{bi} - T_{be}\right)}{\rho r_i c_{bi}} \bar{q}_i \frac{dt}{dx} \tag{29}$$

which when integrated we have

$$T_{bi}(t) = T_{be}(0) + \left(T_{bi}(0) - T_{be}(0)\right) \exp\left[-\frac{2h_i}{\rho r_i c_{bi}} \int_0^t \bar{q}_i dt\right] \tag{30}$$

Considering that $C_{sbi} = \frac{C_s}{\rho_{bi} c_{bi}}$, Eq. (29) can be written in dimensionless form as

$$\frac{dT_{bi}}{\left(T_{bi} - T_{be}\right)} = \frac{-2Bi_i C_{sbi} \bar{q}_i dFo}{R_1^2} \tag{31}$$

and when integrated we have

$$\theta_i(Fo)=\theta_{e0}+(\theta_{i0}-\theta_{e0})\exp\left[\frac{-2Bi_iC_{sbi}}{R_1^2}\int_0^{Fo}\bar{q}_i dFo\right] \quad (32)$$

Where $\theta_i(Fo)=\frac{T_{bi}(t)-T_m}{T_m}$, $\theta_{i0}=\theta_i(0)=\frac{T_{bi}(0)-T_m}{T_m}$, $\theta_{e0}=\theta_e(0)=\frac{T_{be}(0)-T_m}{T_m}$

In a similar manner one can treat the external fluid and the PCM as shown in Fig. 6. The energy balance results in

$$\dot{m}_{be}c_{be}T_{be}\big|_x+\dot{q}_e dx-Adx\rho_e c_{be}=\dot{m}_{be}c_{be}\left(T_{be}\big|_x+\frac{dT_{be}}{dx}dx\right) \quad (33)$$

which after some mathematical manipulations becomes

$$\dot{m}_{be}c_{be}\frac{dT_{be}}{dx}=\dot{q}_e \quad (34)$$

where $\dot{m}_{be}=A\rho v=\rho_e\pi(r_t^2-r_e^2)\bar{u}_e$, $\dot{q}_e=-2\pi r_e k\frac{\partial T}{\partial r}\Big|_{r_e}$

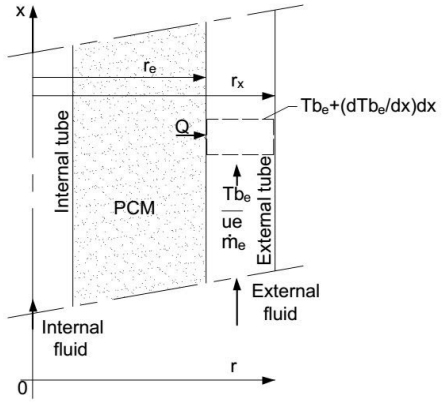

Fig. 6 Details of the flow and phase change problem for the external fluid.

The dimensionless heat flow rate to the external fluid is

$$\bar{q}_e=\frac{\dot{q}_e}{\dot{q}_{\max}}=\frac{\dot{q}_e}{2\pi r_e h_e(T_{bi}-T_{be})} \quad (35)$$

and after some manipulations, one can write

$$\frac{dT_{be}}{dx}=\frac{\dot{q}_e}{\dot{m}_{be}c_{be}}=\frac{1}{\rho_e\pi(r_t^2-r_e^2)\bar{u}_e}\frac{1}{c_{be}}\dot{q}_e \quad (36)$$

and by using Eq. (35) and $\bar{u}_e=\frac{dx}{dt_e}$, one can write

$$\frac{dT_{be}}{dx}=\frac{2r_e h_e(T_{bi}-T_{be})}{\rho_e(r_t^2-r_e^2)c_{be}}\bar{q}_e\frac{dt_e}{dx} \quad (37)$$

which when integrated results in

$$T_{be}(t)=T_{be}(0)+(T_{bi}(0)-T_{be}(0))\exp\left[\frac{2r_e h_e}{\rho_e(r_t^2-r_e^2)c_{be}}\int_0^t\bar{q}_e dt_e\right] \quad (38)$$

Using the dimensionless parameters Fo_e and C_{sbe} in the form:

$$Fo_e=\frac{k_s t_e}{C_s(r_t^2-r_e^2)},\quad C_{sbe}=\frac{C_s}{\rho_{be}c_{be}}$$

and substituting in the Eq. 37 we have

$$\frac{dT_{be}}{dx}=2Bi_e Csb_e(T_{bi}-T_{be})\bar{q}_e\frac{dFo_e}{dx} \quad (39)$$

From Eq. 30 and 39 we have

$$\frac{dT_{bi}}{dx}-\frac{dT_{be}}{dx}=-2(T_{bi}-T_{be})\left[\frac{Bi_iC_{sbi}\bar{q}_i}{R_1^2}\frac{dFo}{dx}+Bi_eCsb_e\bar{q}_e\frac{dFo_e}{dx}\right] \quad (40)$$

The relation between Fo and Fo_e is given by

$$Fo_e(R_3^2-R_2^2)=Fo\frac{t_e}{t_i}\ \text{where}\ R_3=\frac{r_t}{\left(r_e^2-r_i^2\right)^{1/2}} \quad (41)$$

The ratio of the fluid flow velocities is U

$\bar{U}=\frac{\bar{u}_e}{\bar{u}_i}=\frac{t}{t_e}$, which when used together with Eq. 41 one obtains

$$Fo_e(R_3^2 - R_2^2)\overline{U} = Fo \tag{42}$$

and

$$dFo = (R_3^2 - R_2^2)\overline{U}\,dFo_e$$

Eq. (40) can be written in terms of dFo as

$$\frac{dT_{bi}}{dx} - \frac{dT_{be}}{dx} = -2(T_{bi} - T_{be})\left[\frac{Bi_i C_{sbi}\overline{q}_i}{R_1^2}\frac{dFo}{dx} + \frac{Bi_e Csb_e \overline{q}_e}{\overline{U}(R_3^2 - R_2^2)}\frac{dFo}{dx}\right]$$

which can be arranged in the form

$$\frac{d(T_{bi} - T_{be})}{(T_{bi} - T_{be})} = -2\left[\frac{Bi_i C_{sbi}\overline{q}_i}{R_1^2} + \frac{Bi_e Csb_e \overline{q}_e}{\overline{U}(R_3^2 - R_2^2)}\right]\frac{dFo}{dx} \tag{43}$$

Integration of Eq. (43) yields

$$\theta_e(Fo) = \theta_i(Fo) - (\theta_i(0) - \theta_e(0))\exp\left\{-2\int_0^{Fo}\left[\frac{Bi_i C_{sbi}\overline{q}_i}{R_1^2} + \frac{Bi_e Csb_e \overline{q}_e}{\overline{U}(R_3^2 - R_2^2)}\right]\frac{dFo}{dx}\right\} \tag{44}$$

In order to determine the heat absorbed or liberated by the PCM, one uses Eqs. 32 and 44 to obtain

$$\overline{q}_i = \frac{\dot{q}_i}{\dot{q}_{\max}} = \frac{\dot{q}_i}{2\pi r_i h_i (T_{bi} - T_{be})} = \frac{2\pi r_i k \left.\frac{\partial T}{\partial r}\right|_{r_i}}{2\pi r_i h_i (T_{bi} - T_{be})} = \frac{k}{h_i (T_{bi} - T_{be})}\left.\frac{\partial T}{\partial r}\right|_{r_i}$$

which in the dimensionless form becomes

$$\overline{q}_i = \frac{R_1}{Bi_i}\frac{1}{(\theta_{i0} - \theta_{e0})}\left.\frac{\partial \theta}{\partial R}\right|_{R_1}$$

and by the Eq. 21a, we have

$$\overline{q}_i = \frac{R_1}{Bi_i}\frac{1}{(\theta_{i0} - \theta_{e0})}\frac{Bi_i}{R_1}(\theta - \theta_{i0}) = \frac{(\theta - \theta_{i0})}{(\theta_{i0} - \theta_{e0})} \tag{45}$$

and for the external fluid by means of Eq. 21b we have

$$\overline{q}_e = \frac{R_2}{Bi_e}\frac{1}{(\theta_{i0} - \theta_{e0})}\frac{Bi_e}{R_2}(\theta - \theta_{e0}) = \frac{(\theta - \theta_{e0})}{(\theta_{i0} - \theta_{e0})} \tag{46}$$

To derive the equations for the effectiveness and the NTU we followed the procedure of Shamsundar and Srimivesan [29] in which they related the NTU to the solidified mass fraction, F, through an energy balance between the fluid element and the PCM. For the internal fluid, the equation resulting from the energy balance can be written as

$$\dot{m}_{bi} c_{bi}\frac{dT_{bi}}{dx} = -\dot{q}_i = -2\pi r_i h_i (T_{bi} - T_{be})\overline{q}_i \tag{47}$$

Writing the heat flow rate leaving or entering the storage in terms of the fraction of solidified/melt mass,

$$\dot{q}_i = 2\pi r_i h(T_{bi} - T_{be})\overline{q}_i = \pi\rho_b L(r_e^2 - r_i^2)\frac{dF}{dt}$$

where L is the latent heat and F is the fraction of solidified/melt mass.
Hence, Eq. 47 can be written in the form

$$\dot{m}_{bi} c_{bi}\frac{dT_{bi}}{dx} = -\dot{q}_i = -\pi\rho_b L(r_e^2 - r_i^2)\frac{dF}{dt}$$

which can be rearranged in the form

$$\frac{dF}{dt} = \frac{2\pi r_i h(T_{bi} - T_{be})}{\pi\rho_b L(r_e^2 - r_i^2)}\overline{q}_i \tag{48}$$

Define a new dimensionless variable τ as

$\tau = \frac{k_s(T_m^+ - T_{bi})}{\rho_b L(r_e^2 - r_i^2)}t = Ste.Fo$. Eq. (48) can be written as

$$\frac{dF}{d\tau} = 2Bi_i\frac{(T_{bi} - T_{be})}{(T_m^+ - T_{bi})}\overline{q}_i = 2Bi_i\frac{(\theta_{i0} - \theta_{e0})}{(\theta_m^+ - \theta_{e0})}\overline{q}_i \tag{49}$$

If we multiply and divide both sides of Eq. 48 by k and rearranged it and integrating it we have

$$\int_0^t -\frac{\dot{m}_{bi} c_{bi} k_s}{\rho_b L(r_e^2 - r_i^2)}\frac{dT_{bi}}{dx}dt = \int_0^F \pi k_s dF$$

or

$$-\dot{m}_{bi} c_{bi}\int_0^\tau \frac{dT_{bi}}{(T_m^+ - T_{bi})}\frac{d\tau}{dx} = \pi k_s F \tag{50}$$

As the time for phase change is much more than the time for fluid flow, the temperature of the internal fluid T_{bi}

changes with the time and the axial position and also the heat flux $\dot{q}_i$ and F change with τ, Eq. 50 can be written as

$$\dot{m}_{bi}c_{bi}\frac{d\tau}{dx}=\pi k_s F$$ which can be rearranged in the form

$$\frac{\left(\theta_m^+-\theta_{e0}\right)}{\left(\theta_{i0}-\theta_{e0}\right)}\frac{dF}{\overline{q}_i F}=\frac{2Bi_i\pi k_s}{\dot{m}_{bi}c_{bi}}dx$$

which when integrated yields

$$\int_{F_0}^{F_Z}\frac{\left(\theta_m^+-\theta_{e0}\right)}{\left(\theta_{i0}-\theta_{e0}\right)}\frac{dF}{\overline{q}_i F}=\int_0^Z\frac{2Bi_i\pi k_s}{\dot{m}_{bi}c_{bi}}dx=\frac{2Bi_i\pi k_s}{\dot{m}_{bi}c_{bi}}Z$$

or

$$\int_{F_0}^{F_Z}\frac{\left(\theta_m^+-\theta_{e0}\right)}{\left(\theta_{i0}-\theta_{e0}\right)}\frac{dF}{\overline{q}_i F}=NTU_i \quad (51)$$

The effectiveness can be written as

$$\varepsilon_i=\frac{\dot{m}_{bi}c_{bi}\left(T_{iz}-T_{i0}\right)}{\dot{m}_{bi}c_{bi}\left(T_m^+-T_{i0}\right)}=1-\frac{\left(T_m^+-T_{iz}\right)}{\left(T_m^+-T_{i0}\right)} \quad (52)$$

and following the work of [29], one can write

$$\varepsilon_i=1-\frac{F_Z}{F_0} \quad (53)$$

For the external fluid, one can write similar relations for the NTU_e and ε_e as

$$\int_{F_0}^{F_Z}\frac{\left(\theta_m^+-\theta_{e0}\right)}{\left(\theta_{i0}-\theta_{e0}\right)}\frac{dF}{\overline{q}_e F}=NTU_e \quad (54)$$

$$\varepsilon_e=1-\frac{F_Z}{F_0} \quad (55)$$

3. Numerical Solution

The numerical solution is realized by the discretization of the governing equation and the boundary and initial conditions as described by Patankar [30]. In this method the domain is divided into a number of control volumes each one is associated with a nodal point. The discretization is obtained by integration over the control volume and hence each control volume satisfies the conservation principle and consequently all the domain is satisfied, transforming the differential equation into a system of algebraic equations. Numerical tests were realized in order to optimize the number of points used in the numerical solution. It was found that an axial grid of 10 points, a radial grid of 30 points and time step of 0.01s are sufficient to satisfy the convergence criterion.

4. Results and Discussion

In order to validate the model and the numerical method comparisons between the present results and available numerical and experimental data were realized. Initially, the present model was adapted for the case of finless tube and the predicted results were compared with Sparrow et al. [31, 32] and also with the experimental results. The agreement is good as can be verified from Fig.7.

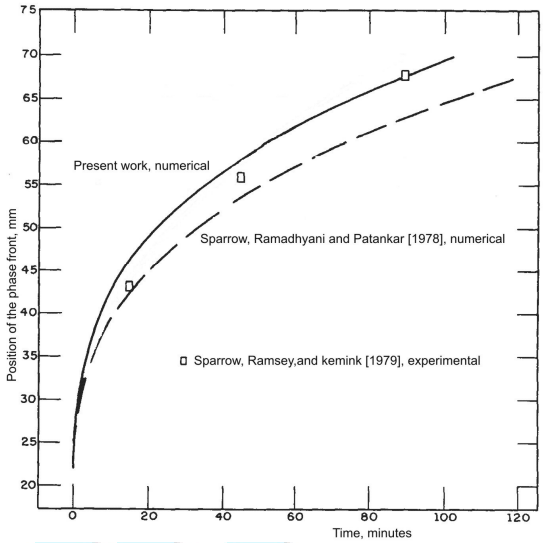

Fig. 7 Comparison of the predicted phase front position with time with available numerical and experimental results from [31, 32] for the case of tube without fins.

Further, for the case of finless tube, the predicted the results for the dimensionless interface position were compared with the results of Sinha and Gupta [33] indicating fairly good agreement as can be verified from Fig. 8.

Additional comparisons were realized for the case of finned tube with the results from [3]. In their study they considered finned tube of constant fin thickness while in the present study, for the sake of facilitating the numerical

calculations the fin was considered as a radial fin and hence its thickness varies along the radial direction. This difference was corrected in our calculation of the solidified fraction. Fig. 9 shows the effect of varying the number of fins on the solidified fraction as predicted from the two models. As can be seen the agreement is good.

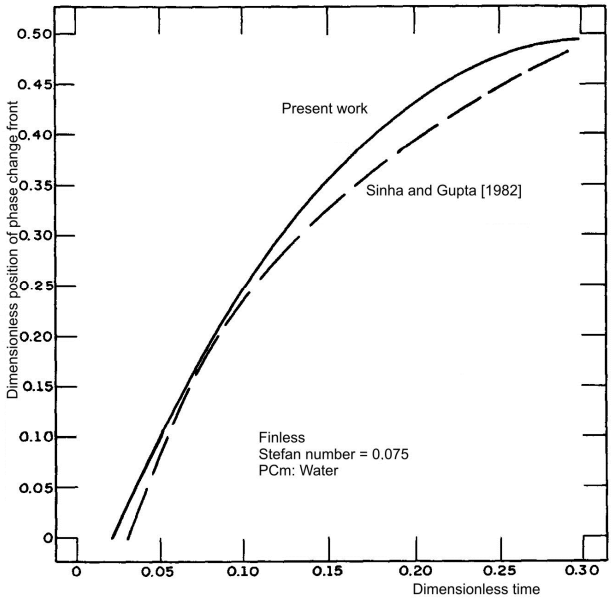

Fig. 8 Comparison of the present predictions of the dimensionless position of the phase front with the results from [33].

Figure 10 shows the effect of varying the fin thickness. As can be seen the thickness of fin effect is small as predicted from the two models. Fig. 11 shows the effect of the fin length of the fin on the solidified mass fraction as predicted from the present study and the study of [3]. As can be seen the agreement between the predictions from the two models is very good.

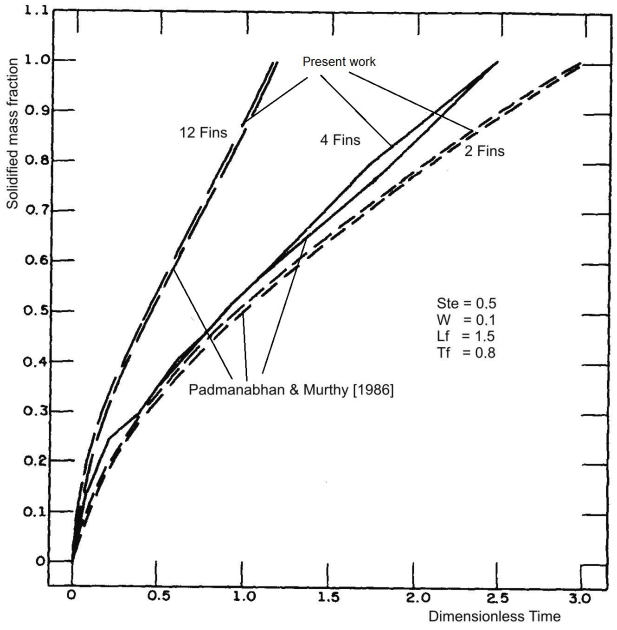

Fig. 9 Comparison of the present numerical predictions of the effect of the number of fins with the results from [3].

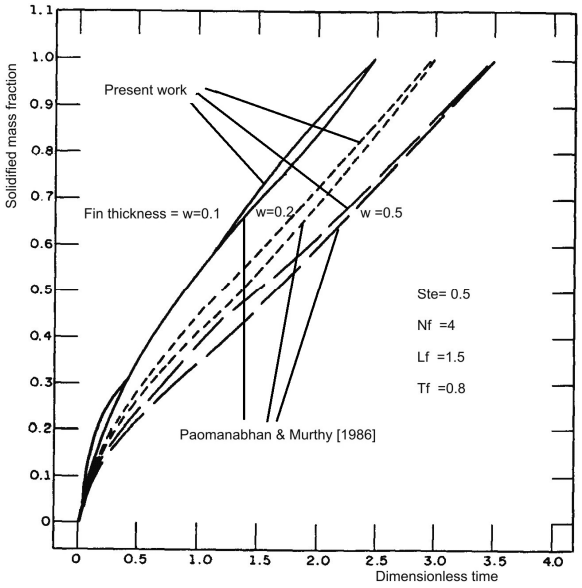

Fig. 10 Comparison of the present numerical predictions of the effect of the fin thickness with the results from [3].

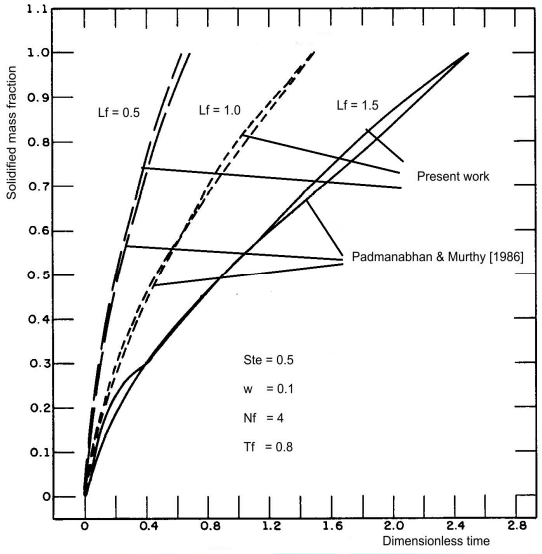

Fig. 11 Comparison of the present numerical predictions of the effect of the fin length with the results from [3].

Additional simulations were realized to investigate the effects of the dimensionless annular gap $R^* = \frac{r_e - r_i}{r_i}$ on the performance of the finned tube. Fig. 12 shows the effects of varying R^* on the solidified mass fraction. As can be seen increasing R^* reduces the solidified mass due to the increase of the thermal resistance caused by the increase of the PCM mass in the annular space. Fig. 13 shows the effect of varying R^* on the effectiveness. As can be seen the effectiveness is found to decrease with the increase of R^*. Fig. 14 shows the effect of varying R^* on the NTU. As can be seen the increase of R^* increases the mass of the PCM and hence increases the NTU of the system.

Based on similar simulations the results are summarized in Fig. 15.
The effects of the dimensionless annular gap on the effectiveness, NTU and the time for complete phase change are shown in Fig.15. Analyzing the above results one can observe that increasing R^* leads to reducing the effectiveness based upon the external or internal fluid since R^* was found to reduce the solidified (melt) mass fraction and to increase the NTU of the system as pointed out before. The effect of R^* is to increase the time for complete solidification. This behavior can be attributed to the increase of the thermal resistance with the increase of the solidified (melt) mass.

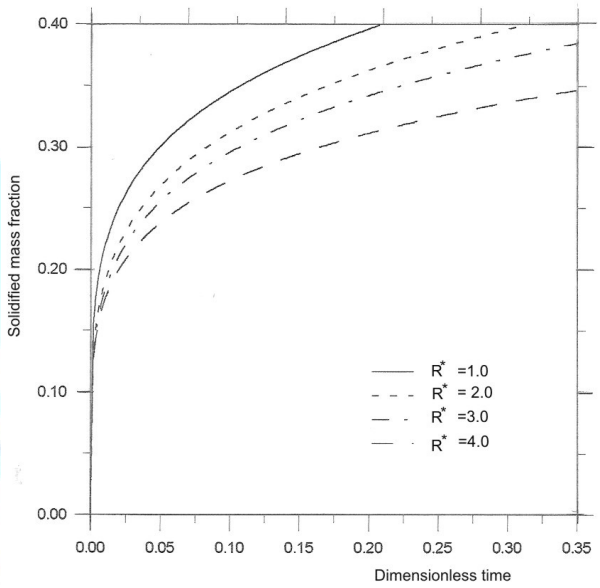

Fig. 12 Effect of the dimensionless gap (R*) on the solidified mass fraction.

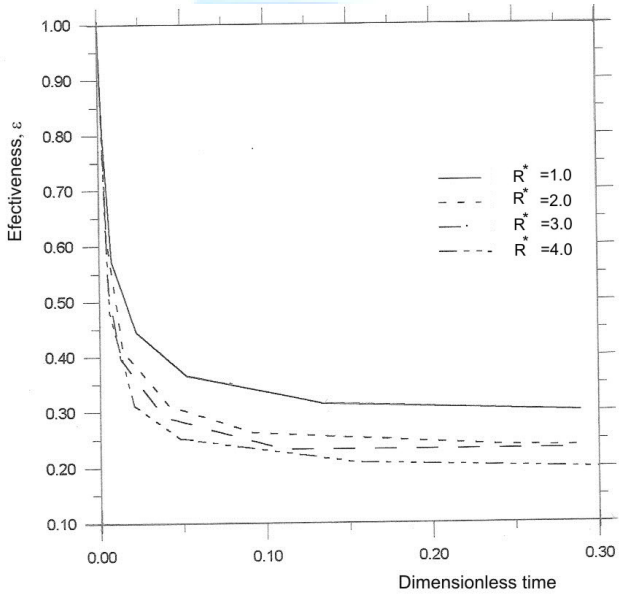

Fig. 13 Effect of the dimensionless gap (R*) on the effectiveness of the system.

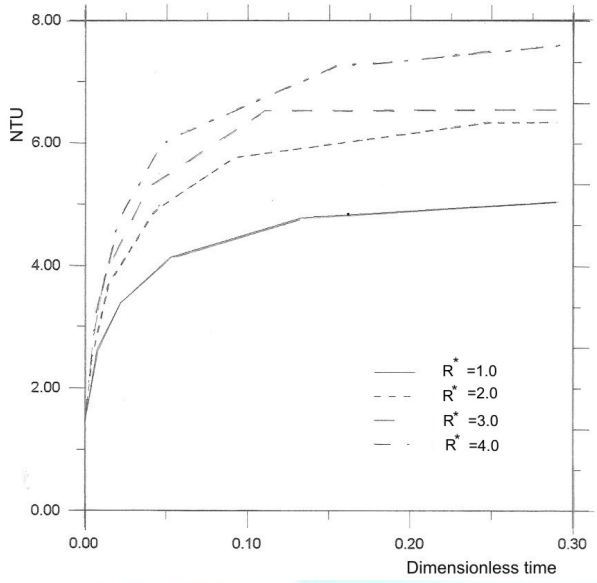

Fig. 14 Effect of the dimensionless gap (R*) on the NTU of the system.

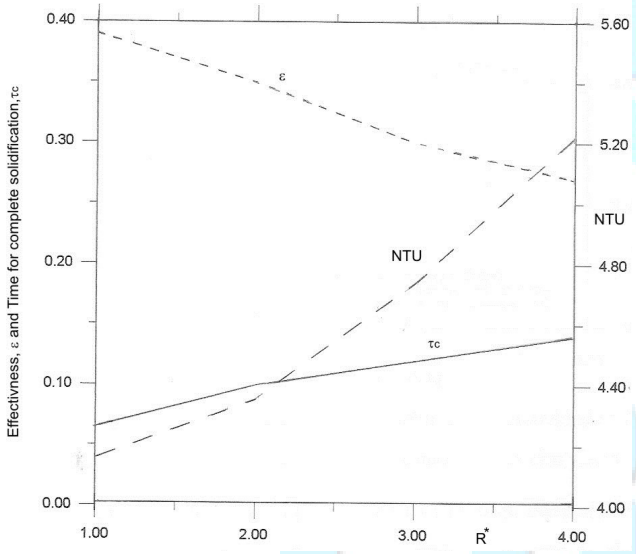

Fig. 15 Effect of the dimensionless gap (R*) on the NTU, effectiveness and time for complete phase change of the system.

Fig. 16 shows the variation of the solidified (melt) mass fraction, the NTU and effectiveness for the case without fins during the phase change process. These simulation results are presented to help demonstrating the beneficial effect of the fins.

The influence of the number of fins on the process of phase change is presented in Fig. 17. One can observe that the solidified mass fraction and the NTU are found to increase with the increase of the number of fins due to the increase of the heat transfer area associated with the fins. Similar behavior to that found in the case of finless tube, the effectiveness is found to decrease with time.

The increase of the fins, radial length is found to have similar effect as that due to increasing the number of fins. Fig. 18 shows that the increase of the fin radial length leads to increase the solidified mass fraction which is caused by the increase of the heat transfer area.

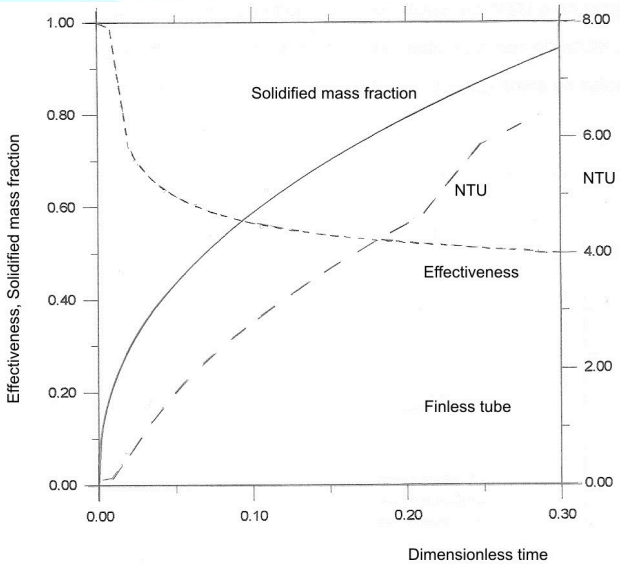

Fig 16 Variation of the NTU, effectiveness and solidified mass fraction with time for the case of finless tube.

4. Conclusions

The proposed model produces results that compare well with available experimental and numerical data. It is found that the increase of the aspect ratio R^* leads to increase the time for complete phase change, increase the NTU and reduce the thermal effectiveness. The number of fins is found to reduce the time for complete phase change, reduce the effectiveness and increase the NTU, while the increase of the fin length is found to increase the solidified mass fraction and reduce the time for complete solidification. The fin thickness seems to have a very small influence on the time for complete solidification, effectiveness and the NTU.

Nomenclature

Latin symbols

A Area of the cross section [m^2]
Bi Biot number = hr/k
C Specific heat [J/kgK]
C(T) Thermal capacity per unit volume [J/m^3K]

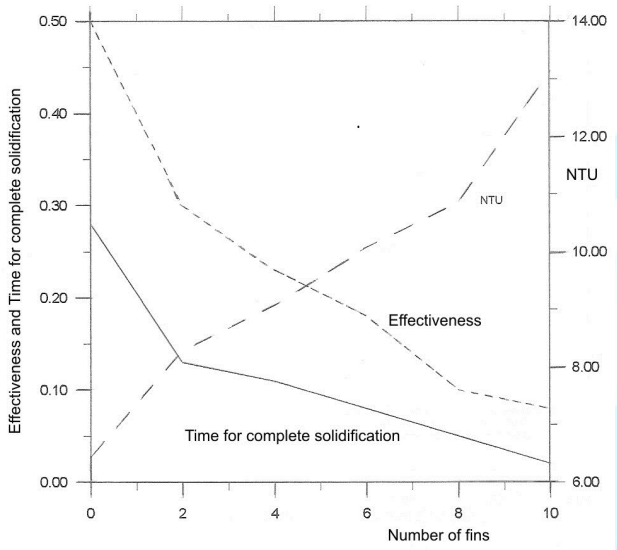

Fig. 17 Effect of the number of fins on the NTU, effectiveness and time for complete phase change of the system.

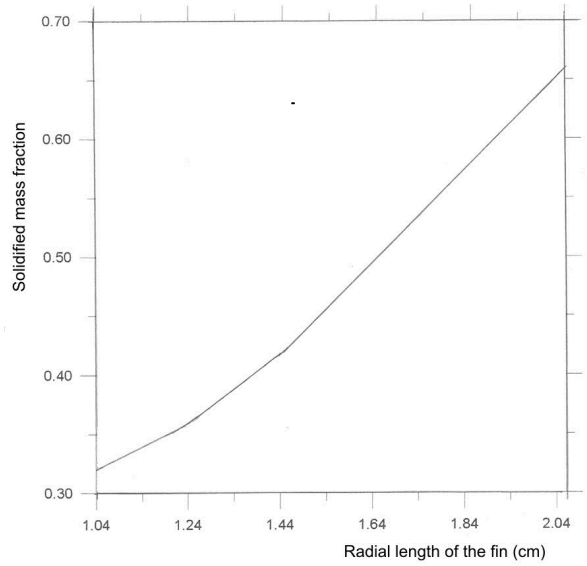

Fig. 18 Effect of the radial fin length on the solidified mass fraction.

$\overline{C}(T)$ Thermal capacity per unit volume including phase change [J/m^3K]
$\tilde{C}(T)$ Equivalent dimensionless heat capacity
f Parameter used in the radial direction
F Solidified mass fraction
Fo Dimensionless time, Fourier number = $k_s t/(C_s(r_c^2 - r_i^2)^{1/2})$
h Convection heat transfer coefficient between the fluid and the PCM [W/m^2K]
g Parameter used in the circumferential direction
H(T) Enthalpy [J/kg]
$\overline{H}(T)$ Enthalpy per unit volume [J/m^3]
k(T) Thermal conductivity [W/mK]
$\overline{k}(T)$ Thermal conductivity including phase change [W/mK]
$\tilde{k}(T)$ Dimensionless thermal conductivity
L Latent heat of the PCM [J/kg]
m Parameter which varies between 0 to 1.
$\dot{m}$ Mass flow rate per unit area [kg/m^2s]
NTU Heat transfer units
NTU_i Number of thermal heat units based on the internal fluid properties
NTU_e Number of thermal heat units based on the external fluid properties
Nu Nusselt number = hd/k
Pr Prandtl number = $c_p\mu/k$
$\dot{q}$ Heat flux per unit length [W/m]
$\dot{q}_{max}$ Maximum heat flux that could be transferred to the fluid per unit length [W/m]
$\overline{q}$ Dimensionless ratio of heat transferred per unit length
r Radius, radial coordenate [m]
R Dimensionless radius, dimensionless coordenate
Re Reynolds number = $\rho vd/\mu$
S_{te} Stefan number = $C_s(T_m^+ - T_{bi}(0))/\lambda$
t Time [s]
T Temperature [K]
T_b Fluid bulk temperature [K]
$\overline{u}$ Average fluid velocity [m/s]
V Control volume
x Position along the tube [m]
$\overline{X}$ Parameter to determine the heat convection coefficient = $(L/D)/(Re.Pr)$
z Axial coordinate [m]
Z Dimensionless axial coordinate

Greek symbols

δ Dirac delta function
Δ Variation
ΔFo Dimensionless time interval
Δϕ Length of the control volume along the circumferential direction
ΔR Length of the control volume along the radial direction
ΔV Control volume
ΔT Half of the phase change temperature range [K]

ε	Effectiveness
ε_i	Effectiveness based on the internal fluid properties
ε_e	Effectiveness based on the external fluid properties
λ	Latent heat per unit volume [J/m^3]
ϕ	Circumferential coordinate [degree]
ϕ_o	Angular start value of the symmetry region [º]
ϕ_e	Angular limit value of the symmetry region [º]
$\eta(u)$	Unitary step function
θ	Dimensionless temperature
θ_a	Half angle of the internal fin thickness [º]
θ_b	Half angle of the external fin thickness [º]
ρ	Specific mass [kg/m^3]
τ	Dimensionless time = S_{te}.Fo
μ	Dynamic viscosity [kg/ms]

Superscript

0	Refers to the preceding time
1	Refers to the present time
+	Refers to the higher limit of the phase change temperature range
-	Refers to the lower limit of the phase change temperature range

Subscript

a	Refers to the fin attached to the internal tube
b	Refers to the fin attached to the external tube
as	Refers to relation fin-PCM
bi	Refers to the to fluid flowing in the internal tube (internal fluid)
be	Refers to the to fluid flowing in the external tube (external fluid)
e	Refers to external side
eo	Refers to the external fluid at the position x=0
h	Refers to the hydraulic diameter
f	Refers to final stage
i	Refers to the internal side
io	Refers to the internal fluid at the position x=0
l	Refers to the liquid state of the PCM
ls	Refers to the relation liquid-solid of the PCM
m	Refers to phase change
s	Refers to the solid state of the PCM
sbi	Refers to the relation between the solid state of the PCM and the internal fluid
sbe	Refers to the relation between the solid state of the PCM and the external fluid
si	Refers to the liquid-solid interface
Z	Dimensionless axial position referring to x=z

Acknowledgments

The authors wish to thank the CNPQ for the doctorate scholarships for the second and third authors and for the PQ Research Grant for the first author.

References

[1] B. Kalhori, S. Ramadhyam, "Studies on heat transfer from a vertical cylinder with or without fins, embedded in a solid phase change medium", Transactions of ASME – Journal Heat Transfer, Vol. 107, 1985, pp. 44-51.

[2] K. Sasaguch, H. Imura, H. Furusho, "Heat transfer characteristics of a latent storage units with a finned tube", Bulletin of JSME, Vol. 29, No. 255, 1986, p. 2978.

[3] P. V. Padmanabhan, M. V. Murthy, "Outward phase change in a cylindrical annulus with axial fins on the inner tube", International Journal of Heat and Mass Transfer, Vol. 29, No. 12, 1986, pp. 1855-1868.

[4] K. A. R. Ismail and C. L. F. Alves, "Analysis of shell-and-tube PCM storage system", Proceedings of the 8th International Heat Transfer Conference, San Francisco, USA, 1989, pp. 1781-1786.

[5] K. A. R. Ismail and M. M. Gonçalves, "Analysis of axially finned PCM storage unit", Proceedings of the Second Renewable Energy Congress, Reading, UK, 1992, Vol. 2, pp. 1041-1045.

[6] J. C. Choi and S. D. Kim, "Heat transfer characteristics of a latent heat storage system using MgCl26H2O", Energy, Vol. 17, No. 12, 1992, pp. 1153-1164.

[7] M. Lacroix, "Study of the heat transfer behavior of a latent heat thermal energy storage unit with a finned tube", Int. J. of Heat and Mass Transfer, Vol. 36, 1993, pp. 2083-2092 http://dx.doi.org/10.1016/S0017-9310(05)80139-5.

[8] J. C. Choi and S. D. Kim, "Heat transfer in a latent heat storage system using MgCl26H2O at the melting point", Energy, Vol. 20, No. 1, 1995, pp. 13-25.

[9] J. C. Choi, S. D. Kim and G. Y. Han, "Heat transfer characteristics in low-temperature latent heat storage systems using salt-hydrates at heat recovery stage", Solar Energy Materials and Solar Cells, Vol. 40, 1996, pp. 71-87.

[10] Y. Zhang and A. Faghri, "Heat transfer enhancement in latent heat thermal energy storage system by using the internally finned tube", International Journal of Heat and Mass Transfer, Vol. 39, 1996, pp. 3165-3173, <http://dx.doi.org/10.1016/0017-9310(95)00402-5>

[11] Velraj, R., Seeniraj, R.V., Hafner, B., Faber, C. and Schwarzer, K., "Heat transfer enhancement in a latent heat storage system", Solar Energy , Vol. 65, 1999, pp. 171-180.

[12] K. A. R. Ismail, J. R. Henriquez, L. F. M. Moura and M. M. Ganzarolli, "Ice formation around isothermal radial finned tubes", Energy Conversion and Management, Vol. 41, 2000, pp. 585-605.

[13] U. Stritih, "An experimental study of enhanced heat transfer in rectangular PCM thermal storage", International Journal of Heat and Mass Transfer, Vol. 47, 2004, pp. 2841-2847. http://dx.doi.org/10.1016/j.ijheatmasstransfer.2004.02.001.

[14] N. Kayansayan, M. Ali Acar, "Ice formatin around a finned-tube heat exchanger for cold thermal energy storage", International Journal of Thermal Sciences, Vol. 45, 2006, pp. 405–418.

[15] N. Yuksel, A. Avci and M. Kilicn, "A model for latent heat energy storage systems", Int. J. Energy Res., Vol. 30, 2006, pp. 1146–1157.

[16] Anica Trp, "An experimental and numerical investigation of heat transfer during technical grade paraffin melting and solidification in a shell-and-tube latent thermal energy storage unit", Applied Thermal Engineering, Vol. 26, 2006, pp. 1830–1839.

[17] A. Erek and M. A. Ezan, "Experimental and numerical study on charging processes of an ice-on-coil thermal energy storage system", Int. J. Energy Res. Vol. 31, 2007, pp. 158–176.

[18] J. Bony, S. Citherlet, "Numerical model and experimental validation of heat storage with phase change materials", Energy and Buildings, Vol. 39, 2007, pp. 1065–1072.

[19] E. B. S. Mettawee, and G. M. R. Assassa, "Thermal conductivity enhancement in a latent heat storage system", Solar Energy, Vol. 81, 2007, pp. 839-845, http://dx.doi.org/10.1016/j.solener.2006.11.009.

[20] S. Wang, A. Faghri, T. L. Bergman, "A comprehensive numerical model for melting with natural convection", International Journal of Heat and Mass Transfer, Vol. 53, 2010, pp. 1986–2000.

[21] F. Rosler and D. Bruggemann, "Shell-and-tube type latent heat thermal energy storage: numerical analysis and comparison with experiments", Heat Mass Transfer, Vol. 47, 2011, pp. 1027–1033, DOI 10.1007/s00231-011-0866-9

[22] M. J. Hosseini, A. A. Ranjbar , K. Sedighi, M. Rahimi, "A combined experimental and computational study on the melting behavior of a medium temperature phase change storage material inside shell and tube heat exchanger", International Communications in Heat and Mass Transfer, Vol. 39, 2012, pp. 1416–1424.

[23] H. Shokouhmand, B. Kamkari, "Numerical Simulation of phase change thermal storage in finned double-pipe heat exchanger", Applied Mechanics and Materials, Vol. 232, 2012, pp. 742-746. http://dx.doi.org/10.4028/www.scientific.net/AMM.232.742

[24] M. R. Anisur, M. H. Mahfuz, M. A. Kibria, R. Saidur, I. H. S. C. Metselaara and T. M. I. Mahlia, "Curbing global warming with phase change materials for energy storage", Renewable and Sustainable Energy Reviews, Vol. 18, 2013, pp. 23–30.

[25] J. N. W. Chiu and V. Martin, "Multistage latent heat cold thermal energy storage design analysis", Applied Energy, Vol. 112, 2013, pp. 1438–1445.

[26] B. Basal, A. Unal, "Numerical evaluation of triple concentric-tube latent heat thermal energy storage", Solar Energy, Vol. 92, 2013, pp. 196-205. http://dx.doi.org/10.1016/j.solener.2013.02.032

[27] A. A. Al-Abidi, S. Mat, K. Sopian, M. Y. Sulaiman, A. T. Mohammad, "Experimental study of melting and solidification of PCM in a triplex tube heat exchanger with fins", Energy and Buildings, Vol. 68, 2014, pp. 33-41, http://dx.doi.org/10.1016/j.enbuild.2013.09.007.

[28] C. Bonacina, G. Comini, A. Fasano, M. Primicerio, "Numerical solution of phase change problems", International Journal Heat and Mass Transfer, Vol.16, 1973, pp. 1825-1832.

[29] N. Shamsundar, R. Srimivesan, "Effectiveness NTU charts for heat recovery from latent heat storage units", Journal Solar Engineering, Vol. 192, 1980, pp. 263-271.

[30] S. V. Patankar, Numerical Heat Transfer and Fluid Flow, Hemisphere Publishing Corporation, Washington, DC, USA. 1980.

[31] E. M. Sparrow, S. Ramadhyani, S. V. Patankar, "Effect of subcooling on cylindrical melting", Transactions of ASME – Journal Heat Transfer, Vol.100, 1978, pp. 395-402.

[32] E. M. Sparrow, J. W. Ramsey, R. G. Kemink, "Freezing controlled by natural convection". Transactions of ASME – Journal Heat Transfer, Vol. 101, 1979, pp. 578-584.

[33] T. K. Sinha, J. P. Gupta, "Solidification in an annulus", International Journal of Heat and Mass Transfer, Vol. 25, 1982, pp. 1771-1773.